Journal of Orthopaedic Surgery and Research

RESEARCH ARTICLE Open Access

NUMB attenuates posttraumatic osteoarthritis by inhibiting BTRC and inactivating the NF-κB pathway

Zhou Lv[1], Yuan Ding[2] and Wei Zhang[1*]

Abstract

Posttraumatic osteoarthritis (PTOA) is closely related to the inflammatory response caused by mechanical injury and leads to joint degeneration. Herein, we aimed to evaluate the role and underlying mechanism of NUMB in PTOA progression. Anterior cruciate ligament transection (ACLT)-induced rats and interleukin (IL)-1β-treated chondrocytes were used as in vivo and in vitro models of PTOA, respectively. The NUMB overexpression plasmid (pcDNA-NUMB) was administered by intra-articular injection to PTOA model rats, and safranin O-fast green staining, the Osteoarthritis Research Society International (OARSI) scoring system, and HE staining were used to evaluate the severity of cartilage damage. The secretion of inflammatory cytokines (TNF-α, IL-1β, and IL-6) and chondrocyte-specific markers (MMP13 and COL2A1) was detected via ELISA. Cell viability and apoptosis were evaluated by MTT and TUNEL assays. NUMB was expressed at lower levels in ACLT-induced PTOA rats and in IL-1β-treated chondrocytes than in control rats and cells. NUMB overexpression enhanced cell viability and reduced cell apoptosis, inflammation and cartilage degradation in chondrocytes stimulated by IL-1β. NUMB bound to BTRC to promote p-IκBα expression, resulting in NF-κB pathway inactivation. BTRC overexpression reversed the promoting effect of NUMB overexpression on cell viability and the inhibitory effects of NUMB overexpression on apoptosis, inflammation and cartilage degradation in IL-1β-induced chondrocytes. In addition, overexpression of NUMB alleviated articular cartilage damage by repressing inflammation and cartilage degradation in ACLT-induced PTOA rats. Our data indicated that NUMB regulated PTOA progression through the BTRC/NF-κB pathway, which may be a viable therapeutic target in PTOA.

Keywords Posttraumatic osteoarthritis, NUMB, BTRC, NF-κB, Inflammation

*Correspondence:
Wei Zhang
18561383547@163.com
[1]Department of Orthopedics, No.971 Hospital of PLA Navy, Qingdao 266071, Shandong, China
[2]Department of Orthopaedics, Qingdao Hospital, University of Health and Rehabilitation Sciences (Qingdao Municipal Hospital), Qingdao 266001, Shandong, China

Introduction

Osteoarthritis (OA) is a common joint disease that can cause chronic progressive joint swelling, pain, joint stiffness and even deformity, thus causing a considerable burden of disability. Its pathogenesis is closely related to the degeneration and destruction of articular cartilage [1]. OA can be divided into two main types: primary OA and secondary OA. Primary OA occurs gradually with age, but the specific etiology of this disease has not been determined. In contrast, secondary OA can be caused by several diseases, such as joint injury, autoimmune inflammatory arthritis, and congenital joint malformation [2]. Posttraumatic osteoarthritis (PTOA) is secondary to OA-induced joint injury and is caused mainly by trauma, bone fracture or overloading, resulting in cartilage or ligament injury [3, 4]. PTOA is prevalent in individuals of any age but is most common in young people following traumatic injury or in the context of unbalanced or excessive load-bearing [5]. Unfortunately, the results of clinical treatment are not ideal for PTOA. Although surgical intervention can reduce the symptoms of PTOA, the incidence of PTOA has not decreased, and there is no ideal measure for treating or preventing PTOA progression [6]. Therefore, for the effective and reasonable prevention and treatment of PTOA, clarifying the mechanism of PTOA and identifying key targets for intervention are highly important.

An increasing number of studies have revealed that cytokines play important roles in the physiological metabolism and functional regulation of organisms. After physical injury to articular cartilage caused by trauma, PTOA chondrocytes release a large number of inflammatory cytokines from focal tissues [7, 8]. These cytokines can regulate the abnormal proliferation or apoptosis of joint chondrocytes; disrupt cartilage tissue metabolism and the synthesis or degradation of the extracellular matrix (ECM); and denature the cartilage matrix, eventually leading to changes in joint cartilage structure or function and interruption of joint activity [9, 10].

NUMB, a conserved membrane protein, is involved in cell fate determination and differentiation. NUMB was originally identified as a mediator of tissue morphogenesis and patterning in the cleavage of Drosophila neurons [11]. A previous study revealed that NUMB could regulate the asymmetric mitosis of cells [12]. In addition, NUMB has been reported to be a tumor suppressor in various cancers. Silencing of NUMB significantly enhanced MCF-7 cell proliferation, invasion and migration via the β-catenin/Lin28 signaling pathway in breast cancer [13]. Shu et al. showed that the expression of NUMB was downregulated in intrahepatic cholangiocarcinoma tumor tissues and closely correlated with poor prognosis in patients with intrahepatic cholangiocarcinoma [14]. Surprisingly, Zhang et al. revealed that NUMB was involved in chondrocyte apoptosis in OA [15]. However, the role and possible molecular mechanism of NUMB in PTOA have not been reported in vivo or in vitro.

In this study, we aimed to determine the expression of NUMB in a rat or cell model of PTOA and explore its possible mechanism in PTOA to identify a potential target for the treatment of PTOA.

Materials and methods

Animals and the PTOA model

Sprague–Dawley rats (male, 8 weeks of age, $n=54$, 220–250 g) were purchased from the Animal Center of Laboratory Animal Center at Beijing Baiaosike Biomedical Technology Co., Ltd. Rats were housed under controlled conditions (25±2 °C, 60% humidity and 12-h light-dark periods). All rats were provided *ad libitum* access to a standard rodent chow diet and filtered tap water. Rats were allowed to acclimate for 1 week prior to the start of any experiments.

As previously reported [15], anterior cruciate ligament transection (ACLT) was performed on the right knee to cause joint instability, thereby inducing PTOA. The rats were randomized into the following four groups ($n=6$ rats/group): a sham group, an ACLT group, an ACLT + vector, and an ACLT + pcDNA-NUMB group. In brief, rats in the final three groups were anesthetized via intraperitoneal injection of sodium pentobarbital. After disinfection, the medial skin of the patellar ligament was incised, and the joint capsule was opened to dislocate the patellar bone. The knee joint was flexed to expose the anterior cruciate ligament, and the anterior cruciate ligament was cut. After rinsing with sterile saline, the wound was closed layer by layer and disinfected, and penicillin was injected intramuscularly to prevent infection. After 6 weeks, the rats were anesthetized with xylazine (5 mg/kg) and ketamine (100 mg/kg), sacrificed by asphyxiation with CO_2 and the knee joints were harvested. All surface soft tissues (skin, muscle, etc.) were removed, and knee joints were fixed in 4% buffered formalin for 48 h at room temperature. Fixed rat knees were decalcified with 10% EDTA solution for 30 days, and the EDTA solution was replaced every 3 days. Then, these specimens were embedded in paraffin and serially cut into 3-μm thick sections for subsequent staining of pathological sections. Besides, the cartilage tissue and blood were immediately removed, t and the latter was collected to prepare the serum for subsequent experiments. In the sham control mice, a skin and capsule incision was instead made. Animal experiments were approved and supervised by the Animal Ethics Committee of No. 971 Hospital of the PLA Navy. All methods were carried out in accordance with relevant guidelines and regulations.

Safranin O/Fast green staining and OARSI scoring

Cartilage tissue sections (n=6 rats/group) were dewaxed with 4% xylene and dehydrated with gradient alcohol. The tissue sections were stained with Fast Green for 10 min and washed with water until the cartilage appeared colorless and was differentiated in acidic ethanol differentiation solution. Then, Safranin O solution (ScyTek, Logan, UT, USA) was used to stain the tissue sections for 30 s, followed by xylene transparency for 5 min and mounting on neutral resin. The presence of any morphological changes in the tissue sections was evaluated in a blinded manner by three certified pathologists using a BX51 optical microscope (Olympus Corp., Tokyo, Japan).

Rat cartilage degeneration in the stained sections was graded using the Osteoarthritis Research Society International (OARSI) scoring system. Specifically, a subjective score of 0–6 was applied as previously described [16]. Scoring criteria were as follows: 0=normal cartilage; 0.5=loss of Safranin-O without structural changes; 1=a small amount of fibrosis but no cartilage loss; 2=surface fissures with a small amount of cartilage loss, 3=fissures and erosions are deep to the calcified cartilage layer and cover less than 25% of the articular surface; 4=fissures and erosions are deep to the calcified cartilage layer and over an area of 25–50% of the articular surface; 5=fissures and erosions are deep to the calcified cartilage layer and over an area of 50–75% of the articular surface; and 6=fissures and erosions are deep to the calcified cartilage layer and cover more than 75% of the articular surface. Three blinded observers graded each section. The three grades for each section were then averaged, and the data for the rat in each group were collated. Higher scores were indicative of more serious cartilage damage.

Hematoxylin-eosin (HE) staining

Cartilage tissue sections (n=6 rats/group) were stained with hematoxylin-eosin (H&E) solution. The percentage of staining-positive area was then determined by pathologists using a BX51 microscope at a magnification of ×400 to evaluate the degree of cartilage injury.

Cell culture

Human primary chondrocytes were purchased from the Cell Bank of the Chinese Academy of Sciences (Shanghai, China). The cells were cultured in complete Dulbecco's modified Eagle's medium (DMEM; Gibco, Grand Island, NY, USA) supplemented with 10% fetal bovine serum (FBS; Gibco, Grand Island, NY, USA), streptomycin (100 mg/mL) and penicillin (100 U/mL) (Sigma, St. Louis, MO, USA) at 37 °C in a humidified atmosphere containing 5% CO_2. Only cells within the fifth passage were used for the subsequent experiments.

Cell treatment

Chondrocytes were harvested as above, counted, and seeded into 96-well plates at a density of 10^4 cells/well (0.1 mL/well). At 24 h postseeding, the cells were treated with various doses of IL-1β (1, 5, or 10 ng/mL; Sigma Aldrich, St. Louis, MO, USA) as a cell inflammatory model, and normal chondrocytes treated with PBS were used as a control.

The short-hairpin NUMB (sh-NUMB) plasmid, short-hairpin BTRC (sh-BTRC) plasmid, and their corresponding negative control (sh-NC), as well as the NUMB and BTRC overexpression plasmids (pcDNA-NUMB and pcDNA-BTRC) and their corresponding negative control (vector), were synthesized by GenePharma (Shanghai, China). Chondrocytes were grown to 70-80% confluence in 24-well plates and then transfected with the above plasmids with Lipofectamine 3,000 reagent (Invitrogen, CA, USA) according to the manufacturer's instructions. After transfection for 48 h, the chondrocytes were collected for subsequent experiments.

3-(4,5-dimethylthiazol-2-yl)-2,5-diphenyltetrazolium bromide (MTT) assay

Cell viability was evaluated using an MTT assay. In brief, after the indicated transfection or treatment, the chondrocytes were harvested, washed with PBS, and counted, after which 1×10^4 chondrocytes were subsequently seeded into 96-well plates. The plates were then incubated at 37 °C for 72 h before each well was treated with 20 μL of 0.5 mg/mL MTT (Beyotime, Shanghai, China) for 4 h. After the supernatant was removed, 150 μL of dimethyl sulfoxide (Sigma Aldrich, St. Louis, MO, USA) was added to each well (Sigma Aldrich, St. Louis, USA). After that, the optical density (OD) was subsequently evaluated at 490 nm using an automated microplate reader (Molecular Devices, San Jose, CA) to determine the number of viable cells.

TdT-mediated dUTP Nick-End labeling (TUNEL) staining

After transfection, TUNEL staining was performed using a TUNEL fluorescence kit (Roche, Basel, Switzerland) to detect apoptosis in chondrocytes in the presence of IL-1β (10 ng/mL). In brief, the chondrocytes were harvested, rinsed with PBS, counted, and seeded onto glass coverslips at 10^3 cells/coverslip. The cells were then fixed by coating each coverslip with acetone/methanol (vol/vol) for 5 min and placing them at -20 °C. Then, the chondrocytes were incubated with equilibration buffer for 10 s before terminal deoxynucleotidyl transferase (TdT) was added for 1 h at 37 °C. Subsequently, the chondrocytes were incubated with the reaction mixture for 60 min, and the cell nuclei were stained with DAPI. The images/slides were observed by using an inverted fluorescence microscope (Nikon, Tokyo, Japan). A visiopharm image

analysis software (Version 6.7.0.2590; Visiopharm, Westminister, CO, USA) was used to count TUNEL-positive stained cells. The number of TUNEL-positive apoptotic chondrocytes are presented as (TUNEL-positive cells)/(total cells)×100%.

Western blotting

Cartilage tissues (50 mg/rat) and transfected chondrocytes were collected and lysed with RIPA buffer containing protease inhibitors (Beyotime, Jiangsu, China). Following the quantitation of protein content using a bicinchoninic acid (BCA) protein assay kit (Beyotime, Shanghai, China), equal amounts of protein (20 μg) were loaded into the wells of a 10% SDS–PAGE gel, and the proteins were resolved. Thereafter, the proteins were electrotransferred to polyvinylidene difluoride (PVDF) membranes (Millipore, Billerica, MA). For each protein of interest, a dedicated blot was generated (this would reduce the risk of antigen loss due to stripping/reprobing one membrane over and over). Nonspecific binding on each membrane was blocked by coating the membrane with a solution of 10 mM Tris-buffered saline (TBS) containing 5% nonfat milk and then incubating the mixture at 25 °C for 2 h. The membranes were incubated with primary antibodies purchased from Abcam (Cambridge, UK), and the antigens used were NUMB (1: 1,000), BTRC (1: 1,000), p-p65 (1:500), p65 (1: 1,000), IκBα (1: 1,000), and p-IκBα (1: 1,000). In all the cases, an antibody against GAPDH (1: 1,000) was also included (as a housekeeping/protein loading protein). All the membranes were then incubated at 4 °C for at least 12 h. Thereafter, each membrane was gently rinsed with TBS containing Tween-20 (TBST), coated with TBST containing horseradish peroxidase-conjugated secondary antibody (1: 5,000) and incubated at room temperature in the dark for another 2 h. Immunoblots were visualized by an enhanced chemiluminescence detection kit (ECL kit; Millipore, Billerica, MA) under a chemiluminescence imaging analysis system (Amersham Imager 600, GE, CT, USA). Relative integrated density values were calculated using ImageJ software provided by the National Institutes of Health (Bethesda, MD, USA).

Immunofluorescence staining

Chondrocytes were inoculated on polylysine-coated cover glass for 24 h, fixed with 4% paraformaldehyde for 20 min, and permeated with PBS containing 0.2% Triton X-100 for 10 min. Then, 5% BSA in PBS was added dropwise to the slides, which were blocked for 30 min at room temperature. Thereafter, the slides were coated with a solution of PBS containing a 1:200 dilution of the primary antibody against NF-κB p65 (Abcam, Cambridge, UK) at 4 °C overnight. The cells were incubated with a PBS solution containing a 1:500 dilution of Alexa Fluor® 555-conjugated secondary goat anti-rabbit antibodies (Cell Signaling Technology, Danvers, USA). The samples were incubated in the dark for 1 h at room temperature before they were gently rinsed with PBS, after which the cells were counterstained with DAPI solution (5 μg/mL) (Beyotime, China) for 10 min. Images were observed by an Olympus fluorescence microscope (Nikon, Tokyo, Japan) to determine the fluorescence intensity with Image-Pro Plus 6.0 (NIH, Bethesda, MD, USA).

Enzyme-linked immunosorbent assay (ELISA)

The levels of TNF-α and IL-6 in the serum and in the supernatants from cultured chondrocytes were measured with commercial ELISA kits (R&D Systems, MN, USA) following the manufacturer's instructions. Similarly, the levels of related secretory proteins, such as MMP-13 and COL2A1, were also detected via ELISA kits (R&D Systems, MN, USA). The limits of detection of the kits were 7.2 pg/TNF-α/mL, 1.8 pg IL-6/mL, and 21.3 pg MMP-13/mL. The level of COL2A1 was detected by sandwich ELISA and an anti-COL2A1 antibody (1: 1,000). All the samples were evaluated in triplicate.

Coimmunoprecipitation (Co-IP) assay

Chondrocytes (1×10^7 total/treatment) were lysed in RIPA buffer (Beyotime, Shanghai, China) following the manufacturer's protocols. After centrifugation at 12,000 rpm for 10 min, the resulting cell supernatant was collected, aliquoted (500 μL), combined with a PBS solution containing mouse anti-human NUMB antibody (1 : 30), anti-human BTRC antibody (1 : 30), or nonspecific IgG (1 : 50) and incubated overnight at 4 °C. Thereafter, the mixture was treated with 50 μL of a kit-provided solution containing protein A/G agarose beads (Takara Biotechnology, Dalian, China), and the sample was then incubated overnight at 4 °C. After this second incubation, the mixture was centrifuged at 3000 rpm for 5 min, and the beads were collected and washed with phosphate-buffered saline (PBS, pH 7.4) three times. The beads were then boiled in loading buffer for 5 min and centrifuged (3000 rpm, 5 min) to allow the adherent proteins to separate from the beads. All precipitated (IP) products were isolated in this manner and subsequently analyzed via Western blotting.

Statistical analysis

All the statistical analyses were performed with SPSS software (version 28.0, IBM Corp., Chicago, IL, USA), and the results are presented as the means±standard deviations (SDs). Student's t test was used for comparisons between two groups, and one-way analysis of variance (ANOVA) was used for comparisons among groups. $P<0.05$ was considered to indicate a statistically significant difference.

Results

NUMB expression was increased in a PTOA rat model and in IL-1β-induced chondrocytes

To test whether NUMB was involved in PTOA progression, a PTOA model was established in rats and chondrocytes. Safranin O/fast green staining was used to evaluate articular cartilage in the PTOA group, and the results showed that the PTOA group had greater knee cartilage loss and matrix degradation than the sham group at different time points (2, 4, and 6 weeks), as evidenced by markedly increased Osteoarthritis Research Society International (OARSI) scores (Fig. 1A and B). Western blotting analysis revealed that NUMB expression gradually decreased with time in the PTOA group (Fig. 1C). Moreover, western blotting also showed that the expression of NUMB was significantly decreased in chondrocytes after treatment with IL-1β in a dose-dependent manner (Fig. 1D).

Overexpression of NUMB suppressed IL-1β-induced chondrocyte injury

Chondrocytes were first transfected with a NUMB overexpression plasmid (pcDNA-NUMB) or a negative control (vector), and then the subsets were treated with 10 ng of IL-1β/mL for 24 h. Western blotting revealed that NUMB levels were significantly a greater in NUMB-overexpressing cells than in cells transduced with only the vector (Fig. 2A). MTT and TUNEL assays revealed that treatment of cells with IL-1β caused a significant decrease in cell viability and an increase in cell apoptosis; however, NUMB overexpression markedly reduced these effects (Fig. 2B and C). In addition, IL-1β caused significant activation of inflammation and degradation of chondrocyte-specific markers. IL-6 and TNF-α secretion was markedly upregulated in chondrocytes in the IL-1β group and downregulated in those in the IL-1β + pcDNA-NUMB group (Fig. 2D). NUMB overexpression reduced IL-1β-mediated the promoting effect on MMP13 secretion and the inhibitory effect on COL2A1 secretion (Fig. 2E and F).

NUMB bound to the BTRC and negatively regulated BTRC expression

To further investigate the function of NUMB, we predicted the potential binding partners of NUMB by using the GeneMANIA tool (http://genemania.org/). The results showed that there was a potential binding relationship between NUMB and BTRC (Fig. 3A). Co-IP assays revealed that both the NUMB and BTRC proteins could be detected by immunoprecipitation with the NUMB antibody or BTRC antibody but not with IgG (Fig. 3B and C), suggesting that NUMB could bind with BTRC in chondrocytes. In addition, upregulation of NUMB significantly decreased BTRC expression in chondrocytes, while silencing of NUMB increased BTRC expression, indicating that NUMB bound to BTRC and negatively regulated BTRC expression in chondrocytes (Fig. 3D).

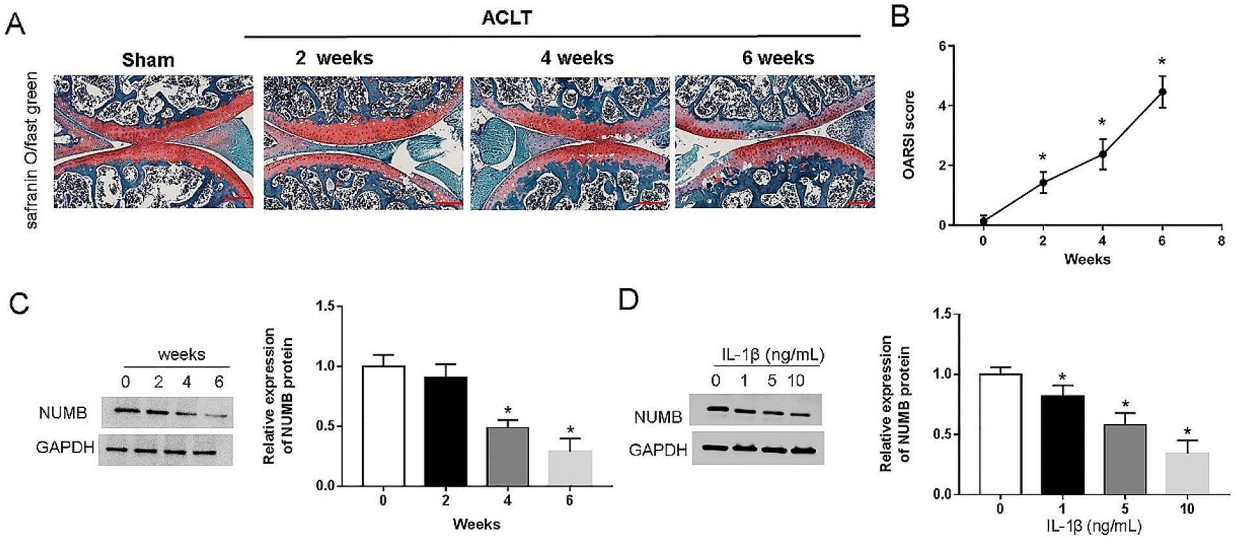

Fig. 1 IL-1β-induced NUMB expression in the knee joint tissue of rats and chondrocytes. (**A**) Safranin O/fast green staining of sagittal sections of knee joint tissue at different time points (2, 4, and 6 weeks). Scale bar = 100 μm. (**B**) The degree of cartilage loss and matrix degradation from 2–6 weeks was calculated using the OARSI scoring system. (C and D) Relative expression of the NUMB protein in the knee joint tissue of rats and in IL-1β-induced chondrocytes was detected via Western blotting. The data are presented as the mean ± SD. *$P < 0.05$

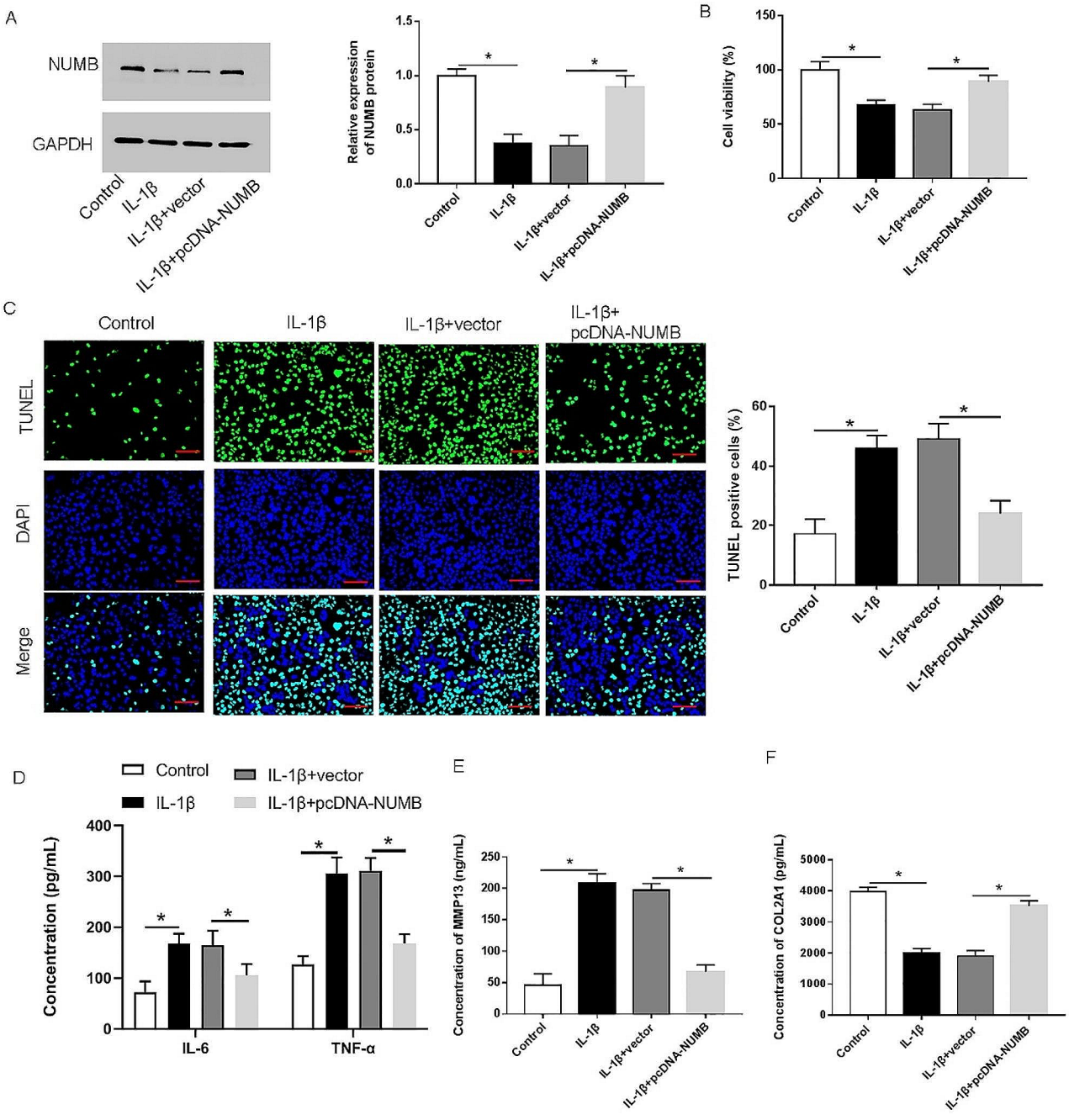

Fig. 2 Effects of NUMB overexpression on chondrocyte viability, apoptosis and inflammation. Chondrocytes were transfected with pcDNA-NUMB (20 nM) or the corresponding negative controls. (**A**) Western blotting detection of NUMB expression in chondrocytes. (**B**) MTT assay detection of cell viability. (**C**) TUNEL staining detection of chondrocyte apoptosis. Scale bar = 100 μm. (D-F) ELISA detection of secretion of IL-6, TNF-α, MMP13, and COL2A1. The data are presented as the mean ± SD. *$P < 0.05$

Overexpression of NUMB suppressed IL-1β-induced chondrocyte injury by downregulating BTRC

To explore whether NUMB exerts its function by binding to BTRC, chondrocytes were transfected with pcDNA-NUMB alone or in combination with pcDNA-BTRC. Western blotting revealed that the expression of BTRC was downregulated by transfection of pcDNA-NUMB but was restored by transfection of pcDNA-BTRC (Fig. 4A). NUMB overexpression elevated cell viability and repressed cell apoptosis in chondrocytes, while BTRC overexpression abrogated these changes (Fig. 4B and C). Additionally, BTRC overexpression significantly reversed the effects of NUMB overexpression on the

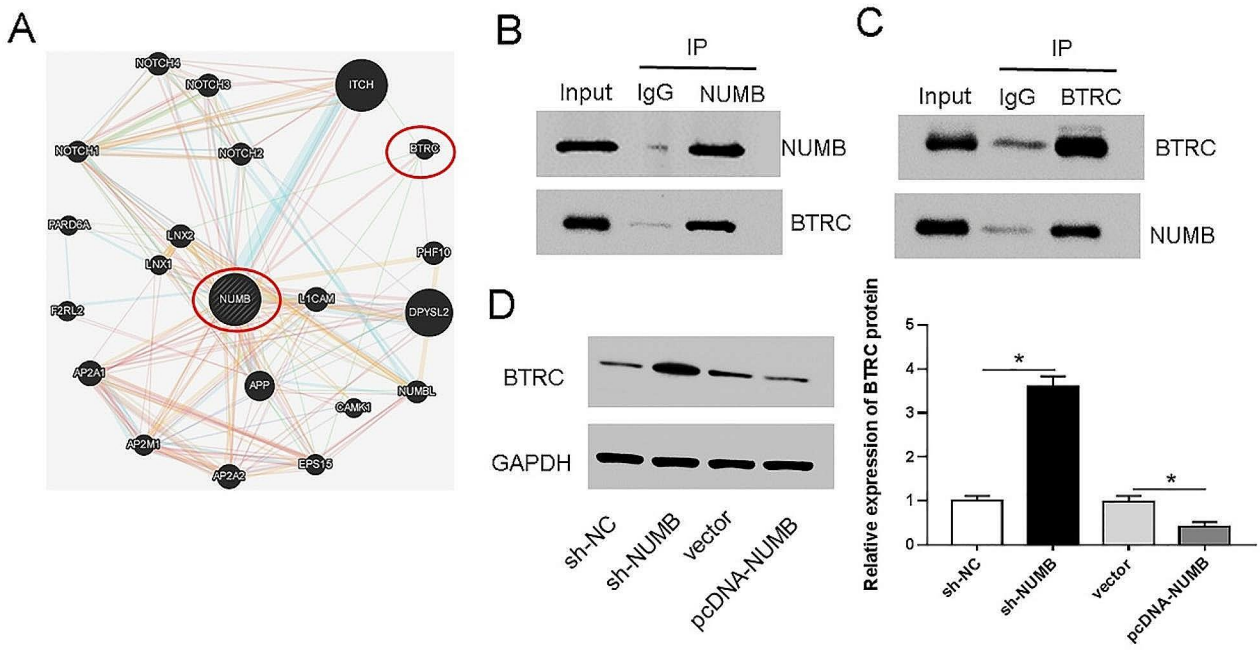

Fig. 3 NUMB binds to BTRC and suppress BTRC expression. (**A**) The online tool GeneMANIA was used to predict the proteins potentially interacting with NUMB. (**B** and **C**) Binding between NUMB and BTRC was detected via co-IP. (**D**) pcDNA-NUMB (20 nM), sh-NUMB (20 nM) and their corresponding negative controls were transfected into chondrocytes. The expression of the BTRC protein was measured via Western blotting. The data are presented as the mean ± SD. *$P < 0.05$

secretion of IL-6, TNF-α, MMP13 and COL2A1 in chondrocytes (Fig. 4D-F).

NUMB blocked the NF-κB signaling pathway via the BTRC/p-IκBα axis

BTRC is reportedly involved in p-IκBα degradation, resulting in the nuclear translocation of NF-κB p65. To verify whether NUMB activated the NF-κB signaling pathway in a BTRC-dependent manner, chondrocytes were transfected with sh-NUMB or pcDNA-NUMB. Western blotting revealed that transfection of sh-NUMB reduced p-IκBα expression and increased p-p65 expression in chondrocytes, while transfection of pcDNA-NUMB increased p-IκBα expression and decreased p-p65 expression (Fig. 5A-C). Immunofluorescence staining revealed that p65 was localized to the nucleus in chondrocytes transfected with sh-NUMB, whereas cytoplasmic p65 was observed in chondrocytes transfected with pcDNA-NUMB (Fig. 5D).

Overexpression of NUMB alleviated articular cartilage degeneration in a PTOA rat model

Western blotting was performed to measure the expression of NUMB in the knee joint tissues of the rats. The expression of NUMB in the ACLT + pcDNA-NUMB group was significantly greater than that in the ACLT + vector group (Fig. 6A and B). Safranin O/fast green staining revealed that NUMB overexpression strongly decreased the severity of articular cartilage degeneration in the PTOA model rats, thus resulting in reduced cartilage OARSI grade (Fig. 6C and D). HE staining revealed that NUMB overexpression improved ACLT-induced chondrocyte damage and exfoliation (Fig. 6E). ELISA revealed a prominent increase in IL-6, TNF-α and MMP13 and a decrease in COL2A1 in the ACLT and ACLT + vector groups compared with those in the sham group, whereas these changes were significantly reversed in the ACLT + pcDNA-NUMB group (Fig. 6F-I). In addition, NUMB overexpression efficiently inhibited the expression of BTRC and p-p65 and promoted the expression of p-IκBα (Fig. 6A, G-L).

Discussion

Posttraumatic osteoarthritis (PTOA) is caused mainly by trauma and accounts for ~ 12% of osteoarthritis (OA) cases; in the body, the knee joint is the most common site of traumatic injury to the body [17, 18]. With the development of PTOA, disability develops and may seriously affect the quality of life of patients. In this study, a rat model of PTOA was established by performing anterior cruciate ligament transection (ACLT) of the right knee joint. In addition, a cell model of PTOA was generated using human chondrocytes treated with IL-1β. In both systems, the data showed that NUMB expression was decreased in the knee joint tissue of rats subjected to ACLT and in that of chondrocytes treated with

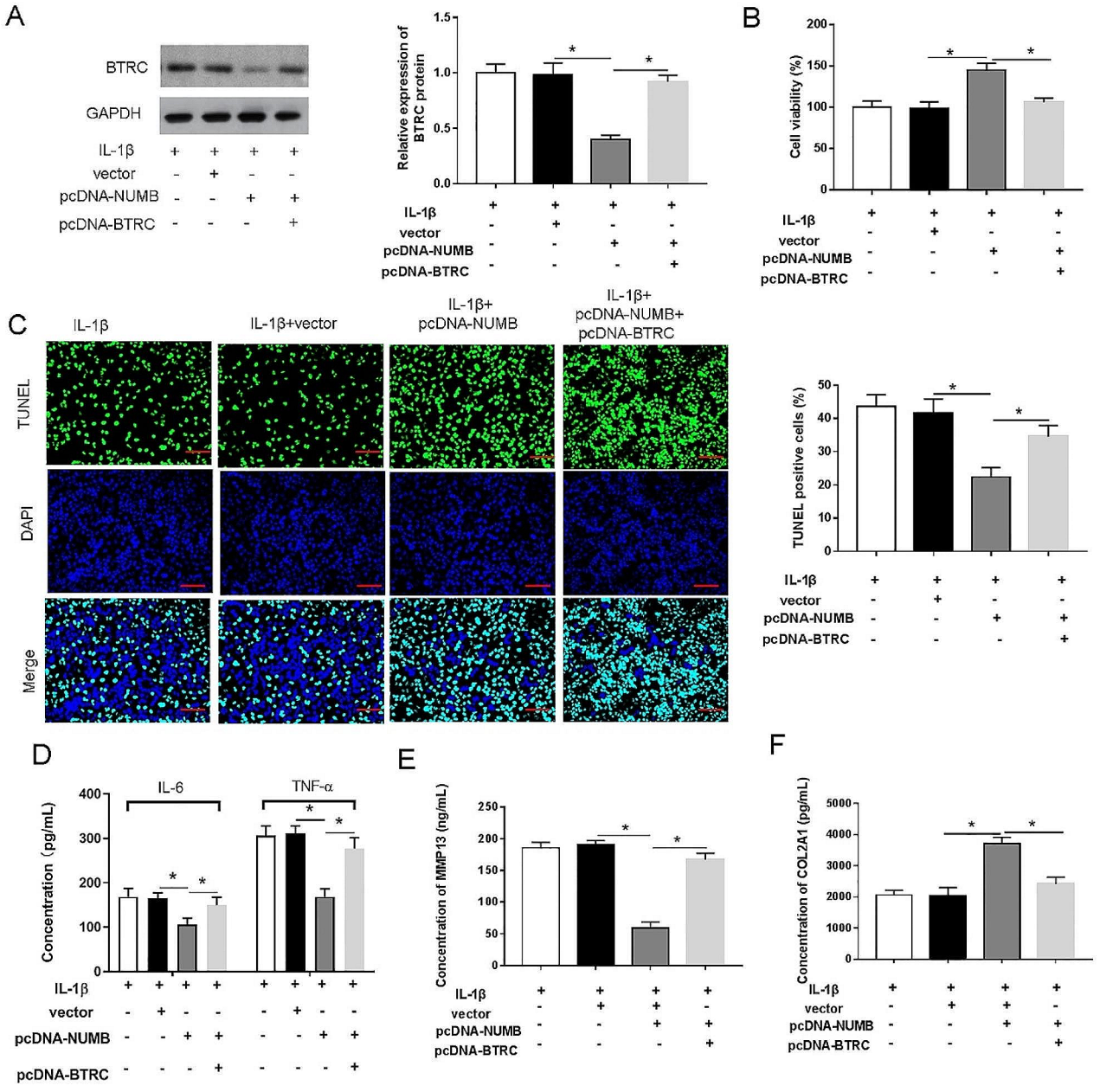

Fig. 4 NUMB promoted cell viability and inhibited apoptosis and inflammation by inhibiting BTRC expression in chondrocytes. Chondrocytes were transfected with pcDNA-NUMB (20 nM) alone or in combination with pcDNA-BTRC (20 nM). (**A**) Western blotting detection of expression of BTRC in chondrocytes. (**B**) MTT assay detection of cell viability. (**C**) TUNEL staining detection of chondrocyte apoptosis. Scale bar = 100 μm. (**D**-**F**) ELISA detection of secretion of IL-6, TNF-α, MMP13, and COL2A1. The data are presented as the mean ± SD. *$P < 0.05$

IL-1β. Surprisingly, NUMB elevation strongly promoted chondrocyte proliferation and reduced chondrocyte apoptosis.

Increasing evidence has shown that the levels of IL-6 and TNF-α in knee joint fluid are ultimately positively related to the severity of PTOA [19]. Matrix metalloproteinase-13 (MMP-13) is an important extracellular matrix-degrading enzyme that can efficiently degrade type II collagen, lead to cartilage degradation and promote the progression of PTAO or OA [20, 21]. Herein, our results showed that the levels of TNF-α and IL-6 were greater in the serum of ACLT-induced rats and IL-1β-induced chondrocytes. The results also revealed a significant increase in MMP13 expression and a decrease in collagen type II alpha 1 chain (COL2A1) expression. Several studies have shown that NUMB participated in regulating the production of proinflammatory cytokines [22]. NUMB has been shown to exert protective effects

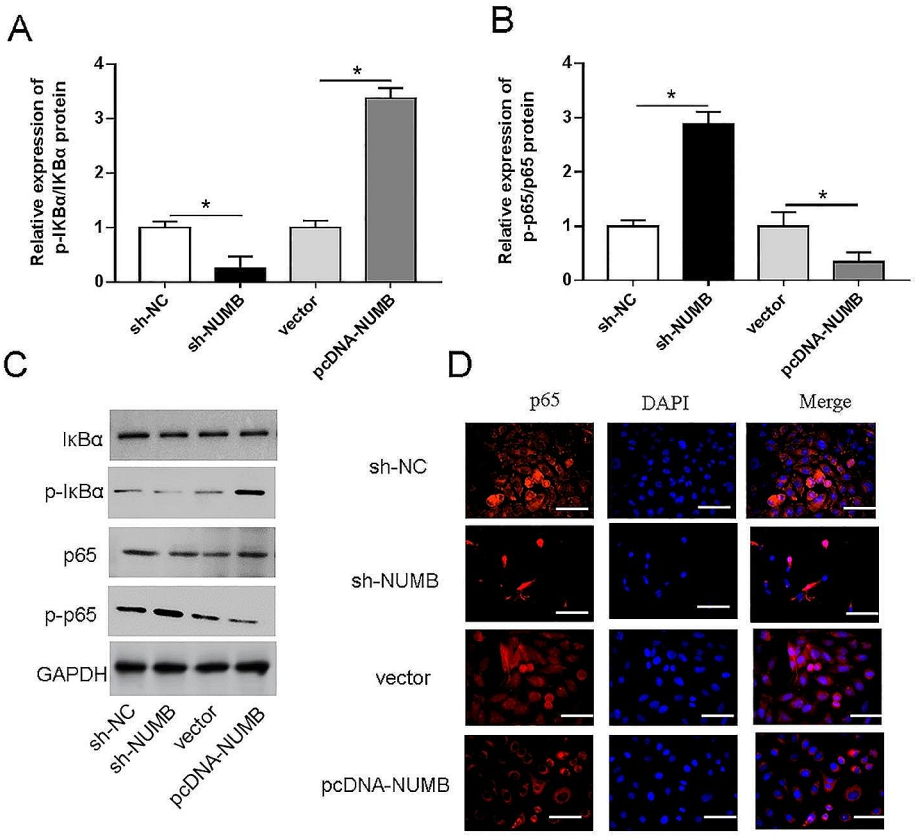

Fig. 5 NUMB inactivates the NF-κB signaling pathway via the BTRC/p-IκBα axis. pcDNA-NUMB (20 nM), sh-NUMB (20 nM) and their corresponding negative controls were transfected into chondrocytes. (**A**-**C**) Western blotting detection of expression of p-IkBα and p-p65 in chondrocytes. (**D**) Immunofluorescence staining detection of nuclear localization of p65 in chondrocytes. Scale bar = 25 μm. The data are presented as the mean ± SD. *$P < 0.05$

on cisplatin-induced acute kidney injury by reducing cisplatin-induced tubular apoptosis and ameliorating tubular necrosis and renal inflammation [23]. Zhou et al. demonstrated that astaxanthin inhibited neuroinflammation by regulating microglial M1 activation through the upregulation of NUMB in lipopolysaccharide (LPS)-treated BV2 cells and mice [24]. Recently, there has been new evidence that the expression of NUMB was significantly downregulated in the cartilage of rat knees after ACLT surgery, and NUMB was a target of miR-146a-5p that could inhibit cell viability and promoted apoptosis and inflammatory factor expression in chondrocytes after IL-1β treatment [15, 25]. Taken together, these results suggest that NUMB has a positive regulatory effect on PTOA. However, the specific mechanism through which NUMB functions during PTOA progression needs further study.

In the present study, beta-transducin repeat containing E3 ubiquitin protein ligase (BTRC) was found to be a potential target of NUMB, and co-IP analysis confirmed the targeting relationship between BTRC and NUMB. At present, research on the BTRC is mostly related to tumors. BTRC, a member of the F-box and WD40 repeat family of proteins, plays an important role in epithelial–mesenchymal transition (EMT) progression [26]. Zhou et al. revealed that BTRC mediated snail ubiquitination in cancer and that BTRC inhibition contributed to the upregulation of Snail expression, which induced EMT [27]. In triple-negative breast cancer, LINC00511 interacted with BTRC to maintain the stability of Snail, thus promoting triple-negative breast cancer cell growth and invasion [28]. Furthermore, recent studies have reported that BTRC mediated the ubiquitination of phosphorylated IκBα (p-IκBα), thereby triggering the translocation of NF-κB to the nucleus and the activation of target genes [29, 30]. Lim et al. showed that WBP2 promoted ubiquitin-mediated proteasomal degradation of IκBα, an inhibitor of NF-κB, by enhancing the mRNA stability of BTRC to promote TNBC cell migration and invasion [31]. TSPAN15 was a novel oncogene that enhanced esophageal squamous cell carcinoma metastasis through the BTRC/NF-KB signaling pathway [32]. Another study showed that miR-10a could accelerate IκBα degradation and NF-κB activation by upregulating BTRC, thus increasing the excessive secretion of NF-κB-mediated inflammatory cytokines and the proliferation and

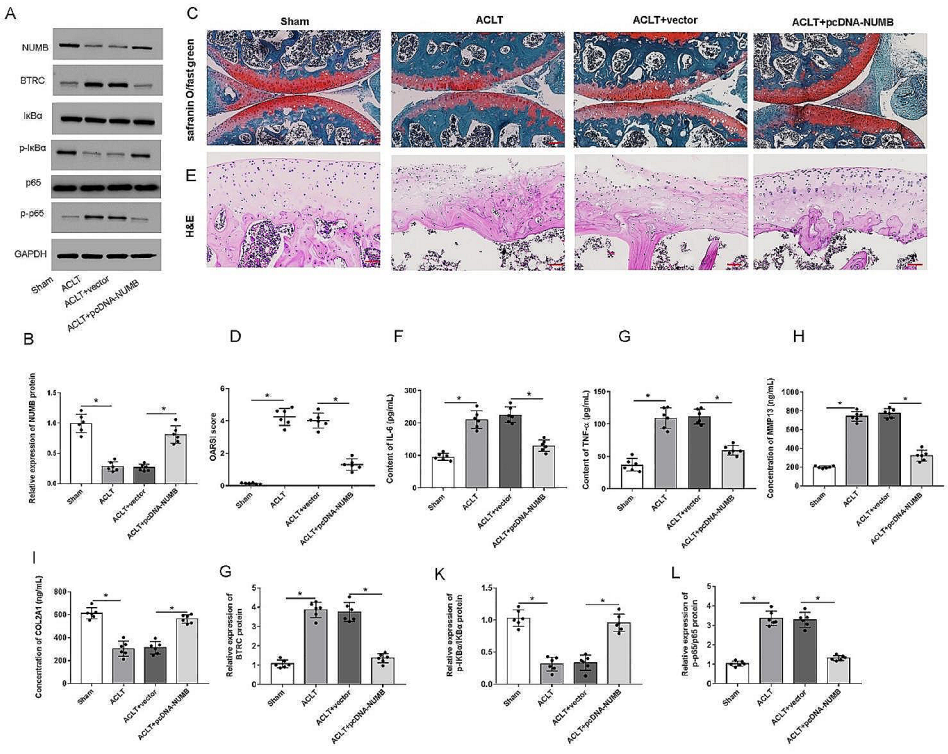

Fig. 6 Overexpressing NUMB inhibited articular cartilage degeneration in a rat model of ACLT-induced PTOA. On Day 3 post-ACLT, the affected knee joints of the rats were injected with a lentivirus encoding a control or NUMB overexpression vector (vector and pcDNA-NUMB). At 6 wk post-ACLT, the rats were euthanized. Sham-operated animals served as negative controls. (**A** and **B**) Western blotting detection of NUMB protein levels in the knee joints of rats. (**C**) Sagittal tibial articular cartilage sections were subjected to safranin O-fast green staining. Scale bar = 100 μm. (**D**) The OARSI scoring system was used to grade mouse cartilage degeneration. (**E**) Chondrocyte damage was assessed using H&E staining. Scale bar = 50 μm. (**F**-**I**) ELISA detection of secretion of IL-6, TNF-α, MMP13, and COL2A1. (A, G-L) Western blotting detection of cartilage expression of BTRC, p-IκBα and p-p65. The data are presented as the mean ± SD. **P* < 0.05

migration of fibroblast-like synoviocytes in rheumatoid arthritis [33]. NF-κB was reported to mediate the production of various inflammatory factors and play a key role in the pathogenesis of PTOA. Inhibition of the NF-κB pathway was able to attenuate cartilage degeneration in a murine model of PTOA [34, 35]. Herein, we found that NUMB inactivated the NF-κB signaling pathway in a BTRC-dependent manner. Overexpression of NUMB reduced BTRC expression and increased p-IκBα expression, resulting in the translocation of NF-κB to the cytoplasm. However, knockdown of NUMB had the opposite effect. BTRC overexpression reversed the effects of NUMB on cell viability, cell apoptosis and inflammation.

Conclusions

In summary, our study demonstrated that NUMB was expressed at lower levels in the knee joint tissue of rats after ACLT surgery and in IL-1β-induced chondrocytes. NUMB downregulated BTRC and inactivated the NF-κB pathway to reduce chondrocyte damage in PTOA. Our results suggested that NUMB might be a further research object for the treatment and intervention of PTOA.

Acknowledgements

This manuscript was submitted as a pre-print in the link "https://doi.org/10.21203/rs.3.rs-1424206/v1".

Author contributions

Zhou Lv and Yuan Ding were responsible for research design. Yuan Ding and Wei Zhang were responsible for conducting the experiments. Zhou Lv and Wei Zhang were responsible for data acquisition and data analysis. Wei Zhang was responsible for writing the manuscript. All the authors have contributed to the completion of this paper.

Funding

None.

Data availability

No datasets were generated or analysed during the current study.

Declarations

Ethical approval

Animal experiments were approved and supervised by the Animal Ethics Committee of Beijing Baiaosike Biomedical Technology Co., Ltd. All methods were carried out in accordance with relevant guidelines and regulations.

Conflict of interest

No conflicts of interest exit in the submission of this manuscript.

Competing interests

The authors declare no competing interests.

Received: 17 April 2024 / Accepted: 30 July 2024
Published online: 23 August 2024

References

1. Lawrence RC, Felson DT, Helmick CG, Arnold LM, Choi H, Deyo RA, Gabriel S, Hirsch R, Hochberg MC, Hunder GG, Jordan JM, Katz JN, Kremers HM, Wolfe F. Estimates of the prevalence of arthritis and other rheumatic conditions in the United States. Part II. Arthritis Rheum. 2008;58(1):26–35.
2. Saleh H, Yu S, Vigdorchik J, Schwarzkopf R. Total knee arthroplasty for treatment of post-traumatic arthritis: systematic review. World J Orthop. 2016;7(9):584–91.
3. Hartlev LB, Klose-Jensen R, Thomsen JS, Nyengaard JR, Boel LWT, Laursen MB, Laurberg TB, Nielsen AW, Steengaard-Pedersen K, Hauge EM. Thickness of the bone-cartilage unit in relation to osteoarthritis severity in the human hip joint. RMD open. 2018;4(2):e000747.
4. Hayami T, Pickarski M, Zhuo Y, Wesolowski GA, Rodan GA, Duong LT. Characterization of articular cartilage and subchondral bone changes in the rat anterior cruciate ligament transection and meniscectomized models of osteoarthritis. Bone. 2006;38(2):234–43.
5. Chery DR, Han B, Li Q, Zhou Y, Heo SJ, Kwok B, Chandrasekaran P, Wang C, Qin L, Lu XL, Kong D, Enomoto-Iwamoto M, Mauck RL, Han L. Early changes in cartilage pericellular matrix micromechanobiology portend the onset of post-traumatic osteoarthritis. Acta Biomater. 2020;111:267–78.
6. Cinque ME, Dornan GJ, Chahla J, Moatshe G, LaPrade RF. High rates of Osteoarthritis develop after anterior cruciate ligament surgery: an analysis of 4108 patients. Am J Sports Med. 2018;46(8):2011–9.
7. Fan L, He Y, Han J, Ybuan P, Guo X, Wang W. The osteoarthritis-associated gene PAPSS2 promotes differentiation and matrix formation in ATDC5 chondrogenic cells. Experimental Therapeutic Med. 2018;16(6):5190–200.
8. He XF, Li W, Zhu LM, Zhang JW. Investigation for effects of iNOS on biological function of chondrocytes in rats with post-traumatic osteoarthritis. Eur Rev Med Pharmacol Sci. 2018;22(21):7140–7.
9. Punzi L, Galozzi P, Luisetto R, Favero M, Ramonda R, Oliviero F, Scanu A. Post-traumatic arthritis: overview on pathogenic mechanisms and role of inflammation. RMD open. 2016;2(2):e000279.
10. Tchetverikov I, Lohmander LS, Verzijl N, Huizinga TW, TeKoppele JM, Hanemaaijer R, DeGroot J. MMP protein and activity levels in synovial fluid from patients with joint injury, inflammatory arthritis, and osteoarthritis. Ann Rheum Dis. 2005;64(5):694–8.
11. Cayouette M, Raff M. Asymmetric segregation of Numb: a mechanism for neural specification from Drosophila to mammals. Nat Neurosci. 2002;5(12):1265–9.
12. Guo M, Jan LY, Jan YN. Control of daughter cell fates during asymmetric division: interaction of Numb and Notch. Neuron. 1996;17(1):27–41.
13. Hu XB, Ouyang LZ, He Y, Xia MZ. Numb confers to inhibit epithelial mesenchymal transition via β-catenin/Lin28 signaling pathway in breast cancer. Exp Mol Pathol. 2019;109:104262.
14. Shu Y, Xu Q, Xu Y, Tao Q, Shao M, Cao X, Chen Y, Wu Z, Chen M, Zhou Y, Zhou P, Shi Y, Bu H. Loss of Numb promotes hepatic progenitor expansion and intrahepatic cholangiocarcinoma by enhancing notch signaling. Cell Death Dis. 2021;12(11):966.
15. Zhang H, Zheng W, Li D, Zheng J. miR-146a-5p Promotes Chondrocyte Apoptosis and Inhibits Autophagy of Osteoarthritis by Targeting NUMB, Cartilage (2021) 19476035211023550.
16. Gerwin N, Bendele AM, Glasson S, Carlson CS. The OARSI histopathology initiative - recommendations for histological assessments of osteoarthritis in the rat. Osteoarthr Cartil. 2010;18(3):S24–34.
17. Bodkin SG, Werner BC, Slater LV, Hart JM. Post-traumatic osteoarthritis diagnosed within 5 years following ACL reconstruction, knee surgery, sports traumatology, arthroscopy. Official J ESSKA. 2020;28(3):790–6.
18. Bailey KN, Furman BD, Zeitlin J, Kimmerling KA, Wu CL, Guilak F, Olson SA. Intra-articular depletion of macrophages increases acute synovitis and alters macrophage polarity in the injured mouse knee. Osteoarthr Cartil. 2020;28(5):626–38.
19. Stannus O, Jones G, Cicuttini F, Parameswaran V, Quinn S, Burgess J, Ding C. Circulating levels of IL-6 and TNF-α are associated with knee radiographic osteoarthritis and knee cartilage loss in older adults. Osteoarthr Cartil. 2010;18(11):1441–7.
20. Neuhold LA, Killar L, Zhao W, Sung ML, Warner L, Kulik J, Turner J, Wu W, Billinghurst C, Meijers T, Poole AR, Babij P, DeGennaro LJ. Postnatal expression in hyaline cartilage of constitutively active human collagenase-3 (MMP-13) induces osteoarthritis in mice. J Clin Investig. 2001;107(1):35–44.
21. Takahashi A, de Andrés MC, Hashimoto K, Itoi E, Otero M, Goldring MB, Oreffo ROC. DNA methylation of the RUNX2 P1 promoter mediates MMP13 transcription in chondrocytes. Sci Rep. 2017;7(1):7771.
22. Kueanjinda P, Roytrakul S, Palaga T. A novel role of Numb as A Regulator of pro-inflammatory cytokine production in macrophages in response to toll-like receptor 4. Sci Rep. 2015;5:12784.
23. Liu Z, Li Z, Chen Z, Li C, Lei L, Wu X, Li Y. Numb ameliorates necrosis and inflammation in acute kidney injury induced by cisplatin. Chemico-Biol Interact. 2020;330:109251.
24. Zhou X, Zhang J, Li Y, Cui L, Wu K, Luo H. Astaxanthin inhibits microglia M1 activation against inflammatory injury triggered by lipopolysaccharide through down-regulating miR-31-5p. Life Sci. 2021;267:118943.
25. Zhao G, Gu W. Effects of miR-146a-5p on chondrocyte interleukin-1β-induced inflammation and apoptosis involving thioredoxin interacting protein regulation. J Int Med Res. 2020;48(11):300060520969550.
26. Zhong J, Ogura K, Wang Z, Inuzuka H. Degradation of the transcription factor twist, an oncoprotein that promotes cancer metastasis. Discov Med. 2013;15(80):7–15.
27. Zhou BP, Deng J, Xia W, Xu J, Li YM, Gunduz M, Hung MC. Dual regulation of snail by GSK-3beta-mediated phosphorylation in control of epithelial-mesenchymal transition. Nat Cell Biol. 2004;6(10):931–40.
28. Liu R, Wang L, Gan T, Pan T, Huang J, Bai M. Long noncoding RNA LINC00511 promotes cell growth and invasion in triple-negative breast cancer by interacting with snail. Cancer Manage Res. 2019;11:5691–9.
29. Orian A, Gonen H, Bercovich B, Fajerman I, Eytan E, Israël A, Mercurio F, Iwai K, Schwartz AL, Ciechanover A. SCF(beta)(-TrCP) ubiquitin ligase-mediated processing of NF-kappaB p105 requires phosphorylation of its C-terminus by IkappaB kinase. EMBO J. 2000;19(11):2580–91.
30. Hatakeyama S, Kitagawa M, Nakayama K, Shirane M, Matsumoto M, Hattori K, Higashi H, Nakano H, Okumura K, Onoé K, Good R.A., N K. Ubiquitin-dependent degradation of IkappaBalpha is mediated by a ubiquitin ligase Skp1/Cul 1/F-box protein FWD1. Proc Natl Acad Sci U S A. 1999;96(7):3859–63.
31. Lim YX, Lin H, Chu T, Lim YP. WBP2 promotes BTRC mRNA stability to drive migration and invasion in triple-negative breast cancer via NF-κB activation, Molecular oncology (2021).
32. Zhang B, Zhang Z, Li L, Qin YR, Liu H, Jiang C, Zeng TT, Li MQ, Xie D, Li Y, Guan XY, Zhu YH. TSPAN15 interacts with BTRC to promote oesophageal squamous cell carcinoma metastasis via activating NF-κB signaling. Nat Commun. 2018;9(1):1423.
33. Mu N, Gu J, Huang T, Zhang C, Shu Z, Li M, Hao Q, Li W, Zhang W, Zhao J, Zhang Y, Huang L, Wang S, Jin X, Xue X, Zhang W, Zhang Y. A novel NF-κB/YY1/microRNA-10a regulatory circuit in fibroblast-like synoviocytes regulates inflammation in rheumatoid arthritis. Sci Rep. 2016;6:20059.
34. Yan H, Duan X, Pan H, Akk A, Sandell LJ, Wickline SA, Rai MF, Pham CTN. Development of a peptide-siRNA nanocomplex targeting NF- κB for efficient cartilage delivery. Sci Rep. 2019;9(1):442.
35. Lin C, Shao Y, Zeng C, Zhao C, Fang H, Wang L, Pan J, Liu L, Qi W, Feng X, Qiu H, Zhang H, Chen Y, Wang H, Cai D, Xian CJ. Blocking PI3K/AKT signaling inhibits bone sclerosis in subchondral bone and attenuates post-traumatic osteoarthritis. J Cell Physiol. 2018;233(8):6135–47.

Publisher's Note